

# Near Surface Phase Transition of SrTiO<sub>3</sub> Studied with Zero Field $\beta$ -Detected Nuclear Spin Relaxation and Resonance

Z. Salman,<sup>1</sup> R.F. Kiefl,<sup>1,2,3</sup> K.H. Chow,<sup>4</sup> M.D. Hossain,<sup>2</sup> T.A. Keeler,<sup>2</sup> S.R. Kreitzman,<sup>1</sup> C.D.P. Levy,<sup>1</sup> R.I. Miller,<sup>1</sup> T.J. Parolin,<sup>5</sup> M.R. Pearson,<sup>1</sup> H. Saadaoui,<sup>2</sup> J.D. Schultz,<sup>2</sup> M. Smadella,<sup>1</sup> D. Wang,<sup>2</sup> and W.A. MacFarlane<sup>5</sup>

<sup>1</sup>TRIUMF, 4004 Wesbrook Mall, Vancouver, BC, Canada, V6T 2A3

<sup>2</sup>Department of Physics and Astronomy, University of British Columbia, Vancouver, BC, Canada V6T 1Z1

<sup>3</sup>Canadian Institute for Advanced Research, Canada

<sup>4</sup>Department of Physics, University of Alberta, Edmonton, AB, Canada T6G 2J1

<sup>5</sup>Department of Chemistry, University of British Columbia, Vancouver, BC, Canada V6T 1Z1

We demonstrate that zero field  $\beta$ -detected nuclear quadrupole resonance ( $\beta$ -NQR) and spin relaxation of low energy  $^8\text{Li}$  can be used as a sensitive local probe of structural phase transitions near a surface. We find that the transition near the surface of SrTiO<sub>3</sub> single crystal occurs at  $T_c \sim 150$  K, i.e.  $\sim 45$  K higher than  $T_c^{\text{bulk}}$ , and that the tetragonal domains formed below  $T_c$  are randomly oriented.

Strontium Titanate (SrTiO<sub>3</sub>) is an ionic insulator with remarkable properties. For example it exhibits “quantum paraelectricity” which can be relieved by oxygen isotope substitution[1]. It is also of significant practical importance as a substrate and buffer layer in electronic heterostructures. At room temperature, bulk SrTiO<sub>3</sub> adopts the cubic perovskite structure, but undergoes an antiferrodisplacive soft-mode structural phase transition to a tetragonal phase at  $T_c^{\text{bulk}} \approx 105\text{K}$ . Intensive research on this second order transition has driven many advances in the general theory of structural phase transitions but has not itself yielded to complete understanding [2]. In SrTiO<sub>3</sub>, and also more generally, differences between the phase transitions occurring in the bulk and those that take place near a free surface are of considerable scientific and technological interest. For example, theoretical calculations predict that the structural and magnetic phase transition temperatures near the surface should be strongly enhanced [3]. There are currently relatively few techniques that can be used to study phase transitions, and in particular those of a structural nature, near the surface at the *local* level. For example, although conventional Nuclear Magnetic Resonance (NMR) and Nuclear Quadrupole Resonance (NQR) are widely used to study condensed matter systems, they generally lack the sensitivity required to investigate surface phenomenon (though notable exceptions exist [4]). However, closely related methods such as beta detected NMR ( $\beta$ -NMR) or NQR ( $\beta$ -NQR) are considerably more sensitive [5, 6, 7, 8], and as a consequence, they are well suited to probe local structural changes near the surface of interesting materials.

In this paper we present zero magnetic field  $^8\text{Li}$   $\beta$ -NQR [6] and spin relaxation measurements near the surface of a single crystal of SrTiO<sub>3</sub>. This study demonstrates, for the first time, that  $\beta$ -NQR can be used as a sensitive local probe of structural phase transitions near a surface. In particular, we find that  $T_c \approx 150$  K near the surface of SrTiO<sub>3</sub>, considerably higher than  $T_c^{\text{bulk}}$ . In addition, we obtain information on the orientation of the near-surface tetragonal domains below  $T_c$ . More generally,

since many other systems [9] produce an appropriate zero field  $\beta$ -NQR signal, we anticipate that our technique is applicable to a wide class of materials.

As discussed in more detail in Ref. [5, 6], the  $^8\text{Li}$  beam is produced at the isotope separator and accelerator (ISAC) at TRIUMF in Vancouver, Canada. It is then spin-polarized using a collinear optical pumping method, yielding nuclear polarization as high as 70%, and subsequently implanted into the SrTiO<sub>3</sub> sample. Since the implanted beam energy (28 keV) is relatively low, the  $^8\text{Li}$  stops at an average depth of  $\sim 1500$  Å. The nuclear polarization, and its time evolution, is the quantity of interest in our experiments. It can be measured through the  $\beta$ -decay asymmetry, where an electron is emitted preferentially opposite the direction of the nuclear polarization at the time of decay [10] and detected by appropriately positioned scintillation counters. The sample is an  $8 \times 10 \times 0.5$  mm single side epitaxially polished (100) single crystal substrate, with RMS surface roughness of 1.5 Å (Applied Technology Enterprises). It was mounted on a coldfinger cryostat in an ultra high vacuum (UHV) environment. Thermal contact between the sample and coldfinger was achieved with a small amount of UHV compatible grease (Apiezon N). The temperature gradient between the sample and diffuser of the cryostat was measured to be less than 0.2 K. The  $^8\text{Li}$  ions were implanted with their initial polarization along the surface of the crystal which is perpendicular to the (100) direction.

Previous measurements at room temperature [6] have established that  $^8\text{Li}^+$  occupies three equivalent face center (F) sites in the cubic SrTiO<sub>3</sub> unit cell, with the Ti<sup>4+</sup> ions at its corners. As a consequence of its location, the local symmetry of the F site is non-cubic even in the cubic phase; therefore, the  $^8\text{Li}$  experiences an almost axially symmetric electric field gradient (EFG),  $V_{ij} = \frac{\partial^2 V}{\partial x_i \partial x_j}$ , with symmetry axis normal to the unit cell face[6, 7]. Since the  $^8\text{Li}$  nucleus has spin  $I = 2$  and an electric quadrupole moment  $Q = +33$  mb, it experiences an electric quadrupole interaction. In zero applied magnetic

field, the spin Hamiltonian is given by:

$$\mathcal{H}_q = h\nu_q[I_z^2 - 2], \quad (1)$$

where  $\nu_q = e^2qQ/8$  and  $eq = V_{zz}$  is the EFG along the symmetry axis. Thus, the  $^8\text{Li}$  nuclear spin polarization,  $\mathbf{p}(t)$ , can be highly sensitive to the details of a structural phase transition at the atomic scale, since one expects such transitions to produce significant changes in the strength and/or symmetry of the EFG tensor. In order to better interpret the results of our measurements, described below, it is useful to keep the following qualitative behavior in mind: (i) a change in the *strength* of the EFG will result in a shift of the resonance frequency, while (ii) a *deviation from axial symmetry* of the  $^8\text{Li}$  site will introduce non-axial components and produce an additional term in the Hamiltonian,

$$\mathcal{H}_\eta = \eta\nu_q(I_x^2 - I_y^2), \quad (2)$$

where  $\eta = (V_{xx} - V_{yy})/V_{zz}$  is the conventional dimensionless EFG asymmetry parameter [11, 12]. Since, in our experiment, most of the  $^8\text{Li}$  are prepared in either the  $|+2\rangle$  or  $|-2\rangle$  spin states,  $\mathcal{H}_\eta$  introduces mixing between the  $|\pm 2\rangle$  spin states with a characteristic frequency splitting  $\Delta_{\pm 2} \simeq 3\eta^2\nu_q$  [6]. This results in a loss of polarization on the timescale of  $1/\Delta_{\pm 2}$ .

First, we discuss the observed temperature dependence of  $\mathbf{p}(t)$  in the  $\text{SrTiO}_3$  sample. The polarization along  $\hat{z}$ ,  $p_z(t)$ , is measured using a method where a pulse of  $^8\text{Li}$  is implanted at a rate of about  $10^6/\text{s}$ , starting at  $t = 0$  for a period  $T = 4$  seconds, and the  $\beta$ -decay asymmetry both during and after the beam period is measured. Measurements of  $p_z(t)$  at different temperatures are shown in Fig. 1. The initial polarization was normalized to its

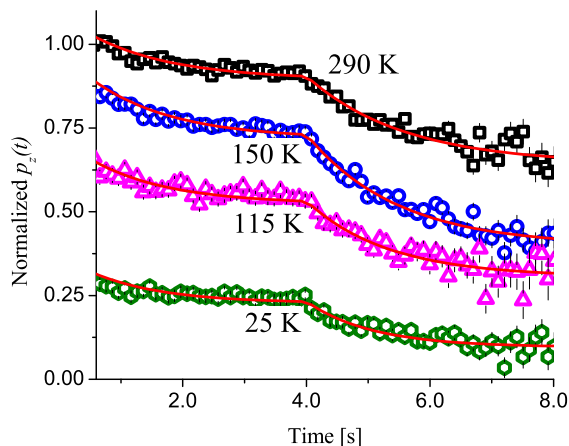


FIG. 1: The polarization as a function of time, normalized to its initial value at  $T = 290$  K, at several temperatures.

value at room temperature.  $p_z(t)$  is determined by both the  $^8\text{Li}$  spin-lattice relaxation rate  $\lambda$  and its radioactive lifetime  $\tau = 1.21\text{s}$ . Assuming a general spin relaxation function  $f(t, t_p : \lambda)$  for the fraction of  $^8\text{Li}$  implanted in

the sample at  $t_p$ , the polarization follows

$$p_z(t) = \begin{cases} \frac{\int_0^t e^{-(t-t_p)/\tau} f(t, t_p; \lambda) dt_p}{\int_0^t e^{-t/\tau} dt} & t \leq T \\ \frac{\int_0^T e^{-(T-t_p)/\tau} f(t, t_p; \lambda) dt_p}{\int_0^T e^{-t/\tau} dt} & t > T. \end{cases} \quad (3)$$

The data in Fig. 1 are fit to Eq. 3 with a phenomenological bi-exponential form,

$$f(t, t_p : \lambda) = A_1 e^{-\lambda_1(t-t_p)} + A_2 e^{-\lambda_2(t-t_p)}. \quad (4)$$

The relaxation rates from the fits are small and do not vary much with temperature. In contrast, as shown in Fig. 2, the initial polarization  $p_z(0)$  exhibits a strong temperature dependence. At high temperatures,  $p_z(0)$  is constant and close to unity. However, it decreases dramatically below 150 K, eventually reaching a temperature independent value of  $\sim 1/3$  below 75 K. As discussed earlier, we attribute the loss of initial polarization to the appearance of non-axial components of the EFG which arise as the crystal's symmetry is lowered below the phase transition. The most striking result in this work is that the loss of polarization in Fig. 2 starts at  $T_c \simeq 150$  K, much higher than  $T_c^{\text{bulk}}$ . We attribute this enhancement of  $T_c$  to proximity to the free surface of the crystal.

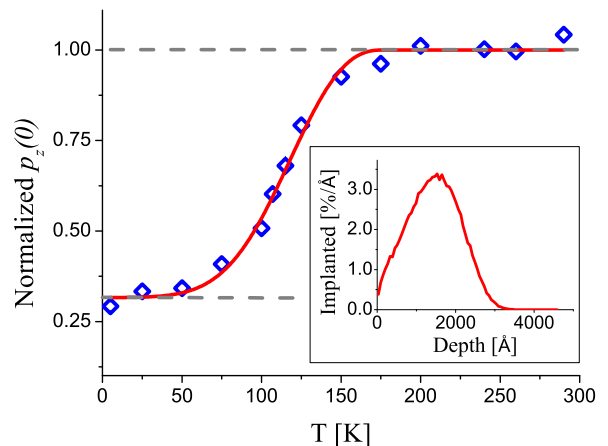


FIG. 2: The normalized initial polarization as a function of temperature. The solid line is a guide to the eye. The inset is the calculated  $^8\text{Li}$  stopping profile.

In order to fully understand the results in Fig. 1 and Fig. 2 one should consider the changes in the local structure around the  $^8\text{Li}$  below the transition, where the lattice parameter  $c$  becomes larger than  $a$  (see inset of Fig. 3). Therefore, two inequivalent  $^8\text{Li}$  sites now exist: those where the  $c$ -axis is perpendicular to the EFG's principal axis ( $F_\perp$ ) and those ( $F_\parallel$ ) where it is parallel. These sites occur in a 2:1 ratio ( $F_\perp:F_\parallel$ ) and hence  $2/3$  of the  $^8\text{Li}$  sites experience non-axial distortions in the EFG. Treating the lattice of  $\text{SrTiO}_3$  as an array of point charges ( $\text{Sr}^{2+}$ ,  $\text{O}^{2-}$  and  $\text{Ti}^{4+}$ ), we calculated  $\eta$  for both types of F site as a function of temperature, using the bulk lattice

constants reported in Ref. [13]. As can be seen in Fig. 3,  $\eta$  is exactly zero for both types in the cubic phase. It remains unchanged through the phase transition for the  $F_{\parallel}$  site, while for the  $F_{\perp}$  sites, it increases up to  $\sim 0.35\%$  due to the tetragonal distortion. The increase in  $\eta$  at  $T_c$  causes an increase in  $\Delta_{\pm 2}$  which is sufficient to produce a partial loss of  $p_z(0)$  due to  ${}^8\text{Li}$  in  $F_{\perp}$  sites.

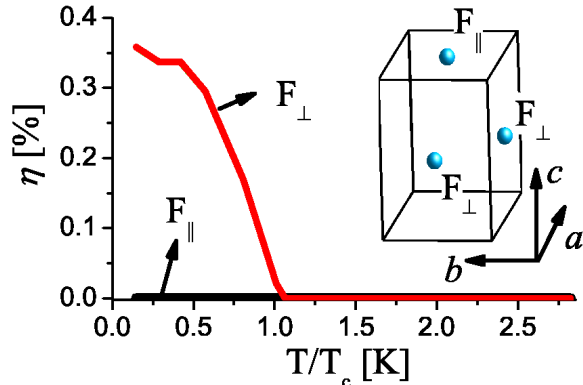


FIG. 3: The calculated  $\eta$  as a function of temperature. The inset shows the different types of  ${}^8\text{Li}$  sites in  $\text{SrTiO}_3$  unit cell.

Additional information, needed to estimate  $\Delta_{\pm 2}$ , can be obtained by measuring the value of  $3\nu_q$  using the nuclear quadrupole resonance, as detailed in Ref.[6]. This was carried from room temperature down to  $\sim 75$  K, below which the resonance could not be observed. Representative spectra at several temperatures are shown in Fig. 4. As can be seen in Fig. 5, the resonance frequency, which occurs at  $3\nu_q$ , increases down to  $\sim 100$  K, below which it appears to saturate. This temperature dependence reflects an increase in the EFG at the  ${}^8\text{Li}$  site, which is consistent with thermal contraction of the  $\text{SrTiO}_3$  lattice, as confirmed by the comparison with simulations using the point charge model. While the absolute value of  $3\nu_q$  obtained from such a simple calculation is generally not expected to agree well with measurements [11], the relative increase in  $3\nu_q$  as a function of temperature (solid lines in Fig. 5) yields very good agreement with the experiment from 290 K down to 105 K. The bifurcation of the calculated values at  $T = 105$  K is due to the bulk phase transition; while the calculated value of  $3\nu_q$  for the  $F_{\parallel}$  site becomes temperature independent, it continues to increase for the  $F_{\perp}$  sites. The experimental results agree with the calculations for the  $F_{\parallel}$  site only, and there is no evidence for a signal from the  $F_{\perp}$  sites. This is further confirmation that below the transition,  $\eta$  for the  $F_{\perp}$  sites becomes significant (see Fig. 3); consequently, the polarization of  ${}^8\text{Li}$  in these sites is lost and does not contribute to the resonance. Note that a typical value of  $3\nu_q \simeq 230$  kHz provides a sufficiently large  $\Delta_{\pm 2}$  for  $\eta$  as low as 0.1% to produce the observed loss of polarization.

It is important to point out that since 2/3 of the polarization of  ${}^8\text{Li}$  stopping in tetragonal domains (where the phase transition has occurred) is lost, the main contri-

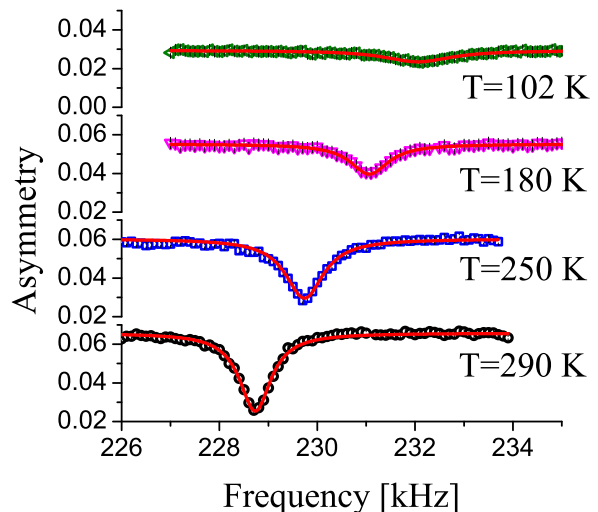


FIG. 4:  ${}^8\text{Li}$   $\beta$ -NQR lines in  $\text{SrTiO}_3$  for different temperatures. The line shifts, broadens and weakens as the sample is cooled from room temperature to 100 K. The solid lines are fits to a Lorentzian, which describes the data very accurately.

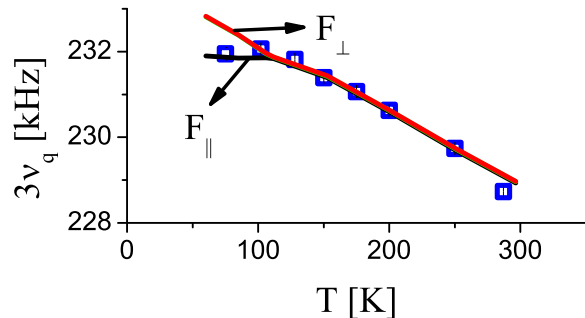


FIG. 5: The resonance frequency,  $3\nu_q$ , as a function of temperature, obtained from fitting the lines to a Lorentzian shape. The solid lines are the calculated value of  $3\nu_q$  from the relative increase of  $\nu_q$  scaled to match the data at 250 K.

tribution to the resonance comes from  ${}^8\text{Li}$  stopping in the cubic phase. Therefore the resonances are less sensitive to the structural phase transition near the surface, since at  $T \gtrsim T_c^{\text{bulk}}$  they will be dominated by  ${}^8\text{Li}$  stopping far from the surface. This is evident from the fact that the calculated resonance frequency, using *bulk* lattice constants, yields good agreement with the experiment (see Fig. 5), and that the resonance amplitude becomes very small below  $T_c^{\text{bulk}}$ .

As mentioned earlier, our observed  $T_c \simeq 150$  K near the surface of  $\text{SrTiO}_3$  is significantly higher than  $T_c^{\text{bulk}}$ , corresponding to a difference of  $\Delta T_c \approx 45$  K. Based on an extrapolation of the penetration depth dependence of the x-ray scattering parameters, an increase of  $\Delta T_c = 220$  K at the surface was predicted [14]. Optical second harmonic generation (SHG) studies recently found that the phase transition near the surface of  $\text{SrTiO}_3$  occurs  $\Delta T_c = 45$  K above the temperature of the bulk phase transition [15]. A similar result was found closer to the surface by elec-

tron diffraction [16]. Unlike these techniques, the  $^8\text{Li}$  nuclei sense the phase transition at the atomic scale, while the net signal is averaged over  $^8\text{Li}$  sites in the implantation volume, which is a beamspot about 3 mm in diameter together with an implantation depth profile. As shown in the inset of Fig. 2, Monte Carlo calculations using the TRIM.SP [17] package predicts that  $^8\text{Li}$  has an average implantation depth of  $\sim 1500$  Å, a width (range straggling) of  $\sim 2000$  Å, and a maximum depth of  $\sim 3000$  Å. Thus the measured  $p_z(t)$  spectra are composed of signals from  $^8\text{Li}$  stopping at varying distances from the surface. The lower symmetry at the surface (together with effects such as surface reconstruction [18]) certainly presents a perturbative influence on the bulk structural phase transition. A simple model of this effect is to assume that  $T_c$  is a monotonically decreasing function of depth, falling from a maximal value  $T_c^{\text{surf}}$  at the surface to  $T_c^{\text{bulk}}$  at large depths. In this picture, the observed breadth of the transition is due, at least in part, to a weighted averaging over the intrinsically inhomogeneous  $T_c$  distribution. The remarkable similarity of our estimate of  $T_c^{\text{surf}}$  to that of the surface-related reflection SHG signal [15] suggests a common intrinsic origin to the enhancement of  $T_c$ .

Finally, since  $p_z(t)$  is strongly dependent on the direction of the  $c$ -axis when the sample undergoes a transition into the tetragonal phase, it provides information on the orientation of the tetragonal domains near the surface. In particular, the observed  $p_z(0)$  is non-zero at low tem-

peratures in the tetragonal phase. This indicates that a fraction of the implanted  $^8\text{Li}$  still experiences an axially symmetric ( $\eta \simeq 0$ ) EFG along its polarization, corresponding to  $^8\text{Li}$  in the  $F_{\parallel}$  site. The observed 1/3 value is strong evidence that the  $c$ -axis of the tetragonal domains is oriented randomly, in agreement with Ref. [19].

In conclusion, we have demonstrated that  $\beta$ -NQR can be used to study structural phase transitions near the surface of  $\text{SrTiO}_3$ . The transition occurs at  $\sim 150\text{K}$ , compared to  $105\text{K}$  in the bulk. The tetragonal domains that are formed at low temperatures were found to be randomly oriented. Analogous studies to those reported here, but at different implantation energies (and therefore stopping depths) will allow depth-profiling of this surface proximity effect. We are currently augmenting our  $\beta$ -NQR spectrometer with a high voltage platform [5] in order to enable such a depth-resolved study. We emphasize that the techniques described in this paper are not restricted to the study of  $\text{SrTiO}_3$ , but should be applicable to investigations of structural phase transitions in many other materials where a nuclear quadrupole interaction is observed [9].

This work was supported by the CIAR, NSERC and TRIUMF. We thank Rahim Abasalti, Bassam Hitti and Donald Arseneau for technical support. We also thank Laura Greene for providing the  $\text{SrTiO}_3$  crystal, W. Eckstein for providing the TRIM.SP code, and K.-C. Chou and W.J.L. Buyers for helpful discussions.

- 
- [1] e.g. see the review J. Dec, W. Kleemann, K. Boldyreva and M. Itoh *Ferroelectrics* **314** 7 (2005).
- [2] R.A. Cowley. *Phil. Trans. R. Soc. London A* **354**, 2799 (1996).
- [3] Structural: K. Binder and P.C. Hohenberg. *Phys. Rev. B* **9**, 2194 (1974); and Magnetic: D.L. Mills. *Phys. Rev. B* **3** 3887 (1971).
- [4] e.g. P.K. Wang, J.P. Ansermet, S.L. Rudaz, Z. Wang, S. Shore, C.P.Slichter and J.H. Sinfelt, *Science* **234**, 35 (1986).
- [5] G.D. Morris, W.A. MacFarlane, K.H. Chow, Z. Salman, D.J. Arseneau, S. Daviel, A. Hatakeyama, S.R. Kreitzman, C.D.P. Levy, R. Poutissou, R.H. Heffner, J.E. Elewski, L.H. Greene and R.F. Kiefl. *Phys. Rev. Lett.* **93**, 157601 (2004).
- [6] Z. Salman, E.P. Reynard, W.A. MacFarlane, K.H. Chow, J. Chakhalian, S.R. Kreitzman, S. Daviel, C.D.P. Levy, R. Poutissou and R.F. Kiefl. *Phys. Rev. B* **70**, 104404 (2004).
- [7] W.A. MacFarlane, G.D. Morris, K.H. Chow, R.A. Baartman, S. Daviel, S.R. Dunsiger, A. Hatakeyama, S.R. Kreitzman, C.D.P. Levy, R.I. Miller, K.M. Nichol, R. Poutissou, E. Dumont, L.H. Greene, and R.F. Kiefl. *Physica B* **326**, 209 (2003).
- [8] e.g. H. Winnefeld, M. Czanta, G. Fahsold, H.J. Jänsch, G. Kirchner, W. Mannstadt, J.J. Paggel, R. Platzler, R. Schillinger, R. Veith, C. Weindel and D. Fick. *Phys. Rev. B* **65**, 195319 (2002); H.D. Ebinger, H.J. Jänsch, C. Polenz, B. Polivka, W. Preyss, V. Saier, R. Veith and D. Fick. *Phys. Rev. Lett.* **76**, 656 (1996).
- [9] Z. Salman, R.F. Kiefl, K.H. Chow, W.A. MacFarlan, S.R. Kreitzman, D.J. Arseneau, S. Daviel, C.D.P. Levy, Y. Maeno and R. Poutissou. *Physica B*, to be published.
- [10] S.G. Crane, S.J. Brice, A. Goldschmidt, R. Guckert, A. Hime, J.J. Kitten, D.J. Vieira, and X. Zhao. *Phys. Rev. Lett.* **86**, 2967 (2001).
- [11] M.H. Cohen and F. Reif. *Solid State Physics* **5**, 321 (1957).
- [12] T.P. Das and E.L. Hahn. *Nuclear Quadrupole Resonance Spectroscopy*. Academic Press Inc., 1958.
- [13] A. Okazaki and M. Kawaminami. *Mat. Res. Bull.* **8**, 545 (1973).
- [14] D.P. Osterman, K. Mohanty and J. Axe. *J. Phys. C* **21**, 2635 (1988).
- [15] E.D. Mishina, T.V. Misuryaev, N.E. Sherstyuk, V.V. Lemanov, A.I. Morozov, A.S. Sigov and Th. Rasing. *Phys. Rev. Lett.* **85**, 3664 (2000).
- [16] N.V. Krainyukova, M.A. Strzhemechny and A.P. Brodyanskii. *Czech. J. Phys.* **46**, 2685 (1996).
- [17] W. Eckstein. *Computer Simulation of Ion-Solid Interactions*. Springer, Berlin, Heidelberg, New York, 1991.
- [18] N. Erdman, K.R. Poeppelmeier, M. Asta, O. Warschkow, D.E. Ellis and L.D. Marks. *Nature* **419**, 55 (2002); J. Zegenhagen, T. Haage and Q.D. Jiang, *Appl. Phys. A* **67**, 711 (1998); K. Johnston, M.R. Castell, A.T. Paxton and M.W. Finnis. *Phys. Rev. B* **70**, 085415

- (2004); B. Stauble-Pumpin, B. Ilge, V.C. Matijasevic, P.M.L.O. Scholte, A.J. Steinfert and F. Tuinstra. *Surf. Sci.* **369**, 313 (1996); G. Koster, G. Rijnders, D.H.A. Blank, H. Rogalla. *Physica C* **339**, 215 (2000).
- [19] A. Buckley, J.P. Rivera and E.K.H. Salje. *J. Appl. Phys.* **86**, 1653 (1999).